# Kinetics of Laser-Heating-Induced Phase Transition of Poly(N-isopropylacrylamide) Chains in Dilute and Semidilute Solutions

Yijie Lu,[†] Xiaodong Ye,*[,†] Junfang Li,[‡] Chunliang Li,[†] and Shilin Liu[†]

[†]Hefei National Laboratory for Physical Sciences at the Microscale, Department of Chemical Physics, University of Science and Technology of China, Hefei, Anhui 230026, China

[‡]State Key Laboratory of Organometallic Chemistry, Shanghai Institute of Organic Chemistry, Chinese Academy of Sciences, 345 LingLing Road, Shanghai 200032, China

ABSTRACT: The kinetics of the phase transition of poly(N-isopropylacrylamide) (PNIPAM) chains from the dilute regime to the semidilute regime was studied by using a homemade fluorescence spectrometer equipped with an ultrafast pulsed infrared laser (width $\sim$10 ns and λ = 1.54 μm). We used 8-anilino-1-naphthalensulfonic acid ammonium salt (ANS) free in water as a fluorescent probe to monitor the conformation changes of the PNIPAM chains. Our results have revealed that in the dilute regime there exists two characteristic transition times that are less than 1 ms, namely, τ_{pearls} ($\sim$0.02 ms), which can be attributed to the nucleation and initial growth of some "pearls" (locally contracting segments) on the chain, and $\tau_{coarsening}$ ($\sim$0.2 ms), which is related to the merging and coarsening of the pearls. At semidilute regime, an extra (third) process ($\tau \sim$ 1.5 ms) appeared, and the contribution from the third process increased with PNIPAM concentration, which can presumably be related to the process of disentanglement of the polymer. A new method to detect the inhomogeneities of the polymer chain segments has been proposed.
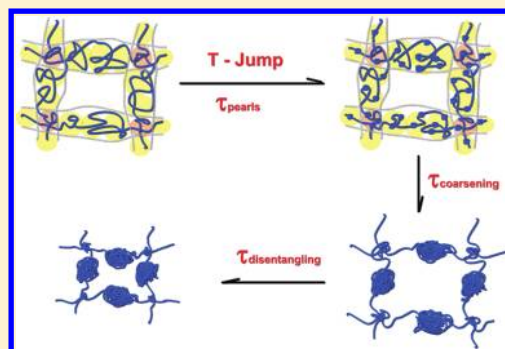
INTRODUCTION

The kinetics of the coil-to-globule transition of thermally sensitive polymer has attracted much attention because of its fundamental role in the understanding of the segment—segment and segment—solvent interactions of polymer chains in solutions. The study of the kinetics of collapsing of polymer chains may help us to understand the protein folding and the packing of DNA.[1-5] Among all the thermally sensitive polymers, poly(N-isopropylacrylamide) (PNIPAM) has been investigated most widely.[6-18] For example, Liu et al. investigated the kinetics of the coil-to-globule transition of a thermally sensitive linear copolymer poly(N-isopropylacrylamide-co-4(1-pyrenyl)butyl acrylate)) (PNIPAM-co-pyrene, M_n = 3.64 × 10^5 g/mol) in water by using a stopped-flow device.[13,14] They found that the chain collapse followed a two-stage kinetics with two characteristic times (τ_{fast} $\sim$ 12 ms and τ_{slow} $\sim$ 270 ms). Note that the stopped-flow technique has been widely used to study the kinetics of micellar formation and protein folding with a time resolution of a few milliseconds. Therefore, it cannot detect the transition faster than $\sim$2 ms. Yushmanov et al. studied the coil-to-globule collapse and intermolecular aggregation of PNIPAM in aqueous solution by temperature-jump ^{1}H NMR spectroscopy.[15] Due to the limitation of the instrument, kinetic behavior on a time scale of less than 1 s cannot be investigated. They concluded that the chain collapse and intermolecular aggregation happen at the most in a few seconds. Tsuboi et al. reported phase separation dynamics of dye-labeled PNIPAM by using laser-induced temperature jump (T-jump) experiments. Their findings reveal one characteristic

time ($\tau \sim$ 0.035 ms).[16] It should be noted that the PNIPAM copolymers used are polydisperse, and the chromophore is hydrophobic, which may bring complexity to the system. More recently, Zhang et al. studied the kinetics of phase transition of PNIPAM in deuterated solution by using a T-jump technique combined with time-resolved midinfrared (MIR) absorbance difference spectroscopy.[17] In order to investigate linear homopolymer chains with a much shorter dead time than milliseconds, such as the mixing time in the stopped-flow methods, we used a fast infrared laser heating pulse to jump the solution temperature and induce the coil-to-globule transition of linear PNIPAM homopolymer chains in water.[18] Our previous results revealed that there exist two characteristic transition times less than 1 ms: τ_{fast} ($\sim$0.1 ms) can be attributed to the nucleation and initial growth of some "pearls" (locally contracting segments) on the chain and τ_{slow} ($\sim$0.8 ms) is related to the merging and coarsening of the pearls.

Until now, to our best knowledge, study on kinetics of the phase transition from dilute regime to semidilute regime in detail has received less attention because of the difficulties in experimental characterization, although protein folding and DNA packing often occur in a concentrated state. Meanwhile, the thermodynamic properties of polymer chains in semidilute solutions have been studied by ultrasensitive differential scanning calorimetry

Table 1. Laser Light Scattering Characterization of PNIPAM Samples Used

sample	M_w (g/mol)	M_w/M_n	$\langle R_g \rangle$ (nm) 25.0 °C	$\langle R_g \rangle$ (nm) 30.4 °C	C^* (mg/mL) calcd[a]	C^* (mg/mL) expt[b]
PNIPAM-1	1.5×10^6	1.5	51	44	7.0	7.3
PNIPAM-2	7.7×10^6	1.4	114	97	3.4	3.0

[a] Calculated by $C^* \sim 3M_w/(4\pi N_A R_g{}^3)$. [b] Measured by present method.

(US-DSC),[19,20] dynamic light scattering (DLS),[21] and fluorescence spectroscopy.[22−24] Zhang et al. has investigated PNIPAM chains in semidilute solutions by US-DSC.[19,20] The study shows different contributions of interchain association and intrachain contraction in dilute and semidilute solutions. As concentration increases, the chains have more chance to undergo interchain association instead of intrachain contraction. Yuan et al. observed one fast and one slow relaxation mode in semidilute aqueous solution of PNIPAM by dynamic light scattering.[21] Their study mainly focused on the origin of the slow relaxation mode. Recently, Tao et al. investigated the interchain contraction and association of polystyrene in semidilute solution near the Θ temperature by using nonradiative energy transfer (NET) because NET is known as a "spectroscopic ruler" for measurement of distance about several nanometers. They observed the real-time conformational changes of polystyrene chains at different solvent conditions, and their results were explained on the basis of the blobs model.[22,23] Duhamel et al. reported the dynamics of poly(N,N-dimethylacrylamide) in semidilute solutions by fluorescence blob model in acetone and dimethylformamide.[24−26] They found the radius of a fluorescence blob was scaled to the number of monomers constituting a fluorescence blob ($N_{F\text{-blob}}$) as $N^\nu{}_{F\text{-blob}}$, where ν equaled 0.66 ± 0.03, which is close to the expected Flory exponent of 0.6.[24] In our present study, by using the laser-induced temperature jump method and water-soluble ANS free in solution as a fluorescent probe due to its sensitivity to its hydrophobic/hydrophilic surroundings,[27] we found that the entanglement of PNIPAM chains has great effects on the kinetics of the collapse process. Our main objective is to understand the roles that chain entanglement played in the chain collapse process.

■ EXPERIMENTAL SECTION

Materials. Details for synthesis of the PNIPAM homopolymer can be found elsewhere.[28] Briefly, monomer N-isopropylacrylamide was recrystallized three times in a benzene/n-hexane mixture. The purified monomer and recrystallized azobisisobutyronitrile (AIBN) as initiator were dissolved in purified solvent benzene. The solution was degassed through three cycles of freezing and thawing and the reaction was carried out at 56 °C for 30 h. The resultant PNIPAM homopolymer was carefully fractionated by the dissolution/precipitation process in a mixture of dry acetone and dry hexane at the room temperature. The weight-average molar mass (M_w), the radius of gyration ($\langle R_g \rangle$) and the hydrodynamic radius ($\langle R_h \rangle$) of two PNIPAM fractions used in our experiments were determined by a combination of static and dynamic light scattering, and the results are summarized in Table 1. The polydispersity index (M_w/M_n) was estimated from the relative width ($\mu_2/\langle\Gamma\rangle^2$) of the line-width distribution [$G(\Gamma)$] measured in dynamic light scattering since
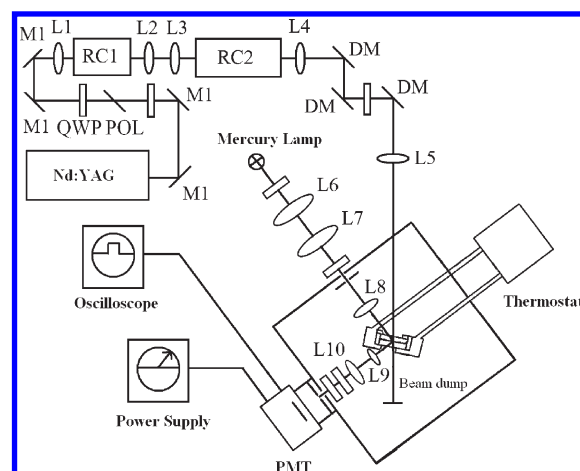

Figure 1. Schematic diagram of our laser temperature-jump instrument: RC1, Raman cell 1; RC2, Raman cell 2; M1, mirror with high reflectance at 1.064 μm; an optical isolator consisted of a thin film polarizer (POL) and a quarter wave plate (QWP) was used to protect the laser from backscattered light; DM, dichroic mirror with high reflectance at 1.54 μm and high transmission at 1.064 μm; L1−L10, lenses. See the details in the text and in ref 29.

$M_w/M_n \sim 1 + 4 \mu_2/\langle\Gamma\rangle^2$. 8-Anilino-1-naphthalensulfonic acid ammonium salt (ANS) was from Fluka with purity ≥97%. A stock of ANS (10.6 mM) solution was prepared. The solution mixtures of PNIPAM and ANS were prepared by adding the stock solution of ANS into different PNIPAM solutions in water with stirring.

Fast Infrared Laser Heating and Fluorescence Detection. The instrument has been described in detail elsewhere.[29] In brief, a pulsed 1.54-μm infrared laser beam (∼6.5 mJ/pulse at 10 Hz, pulse width ∼10 ns) was generated from a Nd:YAG laser (Spectra Physics, Lab-170, repetition rate = 10 Hz) and two Raman shifters (first Stokes shift in CH_4 gas),[30] and the resultant infrared laser was used for the temperature jump experiments because they can be absorbed by the overtone of the O−H stretching vibration in H_2O.[31] The source for excitation of ANS was a 200-W high-pressure mercury lamp (Shanghai Hualun Bulk Factory) with a transmitting filter (245−400 nm). The fluorescence was filtered with a cutoff filter (450 nm), collected with a photomultiplier tube (Hamamatsu R928) and with the standard right angle geometry, and recorded on a Tektronix oscilloscope (TDS 3054B). Each data point was normally averaged over 512 time measurements to improve the signal-to-noise ratio. The oscilloscope itself is fast enough (2 GHz). In our experiment, we used a resistor to gain the electric signal from the photomultiplier tube (PMT). The response time of our setup measured from an oscilloscope depends on the used matched resistor. Adding a larger resistor will certainly increase the signal intensity, but will also increase the response time of the oscilloscope, i.e. the dead time of the oscilloscope. Therefore, in this experiment, by using a 5 kΩ matched resistor instead of a 50 kΩ resistor as in our previous study, we are able to measure the fluorescence or the scattering intensity with a smaller dead time of ∼2 μs compared to that (∼20 μs) in our earlier study.[18,29] The sample cell consisting of a pair of quartz windows with a 200-μm spacer was thermally controlled at 30.4 °C to a precision of ±0.1 °C by a heating bath and the system was stabilized for at least 20 min before each experiment. The cell length of 0.2 mm results in less than 22% absorption of the heating pulses and a
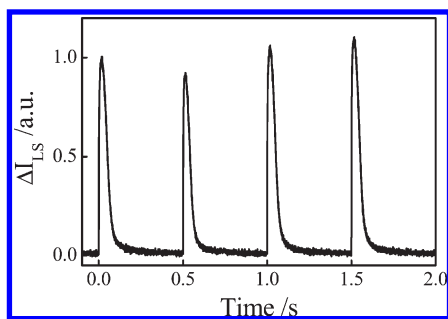
12002

dx.doi.org/10.1021/jp204853p |*J. Phys. Chem. B* 2011, 115, 12001–12006

Figure 2. Time dependence of the light-scattering intensity of PNIPAM-2, where the intensity of the infrared pulsed light was 6.5 mJ, and the concentrations of PNIPAM-2 and ANS were 25.9 mg/mL and 118 μM, respectively, and ΔI_{LS} is defined as $[I_{LS}(t) - I_{LS}(0)]/[I_{LS}(max) - I_{LS}(0)]$.

Figure 3. Temperature dependence of static emission fluorescence spectra of ANS (118 μM) in PNIPAM-2 aqueous solution (5×10^{-4} g/mL), where $\lambda_{ex} = 365$ nm. The inset shows the temperature dependence of fluorescence intensity at wavelength 472 nm for ANS (118 μM) in aqueous PNIPAM-2 solution.

constant temperature jump throughout the cell. Each heating laser pulse jumps the solution temperature from 30.4 to ~33.4 °C, estimated on the basis of the absorption of infrared laser at 1.54 μm and $\Delta T = (I_{IR}/cL)(1 - e^{-2.303AL})$, where I_{IR} is the incident radiation intensity (J·cm^{-2}), c is the heat capacity of the medium in J·cm^{-3}·deg^{-1}, L is the length of the heating path, and A is the medium's absorbance per centimeter. In this study, $c = 4.2$ J·cm^{-3}·deg^{-1}, $L = 0.02$ cm, $I_{IR} = 1.08$ J·cm^{-2}, and $A = 5.3$ cm^{-1}.[31,32] The instrument is schematically shown in Figure 1. Note that the temperature jump (~3 °C) is higher than that in our previous experiment (~2 °C)[18] because of the smaller beam diameter of the infrared laser in our present study. Fluorescence spectra were recorded on a Shimadzu RF-5301PC spectrofluorophotometer by using a quartz cell with an optical path length of 0.5 mm. The temperature of the samples was monitored by an electronic thermometer with a precision of ±0.1 °C.

■ RESULTS AND DISCUSSION

Figure 2 shows the time dependence of the light-scattering intensity of PNIPAM-2 aqueous solution with ANS after the heating laser pulse induced temperature jump, where the concentrations of PNIPAM and ANS were 25.9 mg/mL and 118 μM, respectively. After each heating laser pulse, the intensity of the scattered light instantly increases more than 10 times compared with that before T-jump, which is due to phase transition of the thermally sensitive polymer chains. Note that each heating pulse raised ~3 °C in the scattering volume, which is sufficient to change water from a Θ solvent (~30.4 °C) to a poor solvent and induce the phase transition of PNIPAM solution.[9] We checked the heat dissipation between two infrared laser pulses. Our results showed that when the pulse repetition frequency was reduced from 10 to ~2 Hz by inseting a chopper in front of the sample, the temperature at the laser heating spot can return to 30.4 °C before the next laser pulse, reflecting an identical light scattering intensity before each laser pulse. Note that the PNIPAM-2 solution in Figure 2 is the most concentrated in our whole experiment and PNIPAM-2 has a higher molecular weight than that of PNIPAM-1, which implies it will spend longer time to return to its original state than any other sample after the heating pulse. Therefore, we set the time interval between two heating laser pulses to be 500 ms in our experiments to ensure no residual heating effect and that the unfolding process of PNIPAM will be complete when the next laser pulse comes. Figure 2 also shows that the variation of maximum light scattering intensity is less than ~7%, which indicates the stability of T-jump. Thus, we are
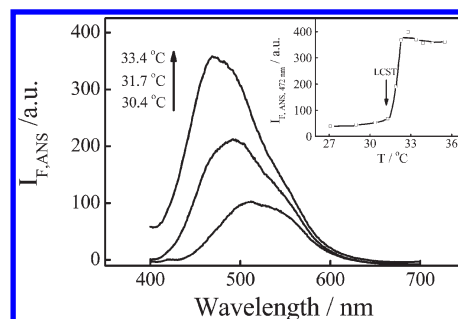
able to repeat the measurements many times and average them to increase the signal-to-noise ratio. It should be noted that "additional hydrogen bond" has been proposed to explain the hysteresis of the phase transition of PNIPAM in aqueous solution in equilibrium state.[33−36] While in our experiments it seems that the dissolution of PNIPAM chains is fast and completes as soon as the heat dissipates. Zhang et al. investigated the association and dissolution of PNIPAM chains from dilute regime to semidilute regime by using ultrasensitive differential scanning calorimetry, and they concluded that less additional hydrogen bonding between PNIPAM segments will form if fast heating rate is used.[19] So one possible reason in our study that hysteresis is not obvious is that the PNIPAM chains do not have enough time to rearrange and form enough hydrogen bonds, as the time that the PNIPAM chains stay as aggregates is as short as ~10 ms and the heating rate is very fast in our experiments.

In our previous study we have shown that when the concentration of PNIPAM is in the dilute regime, there is no significant change in the scattering intensity, i.e., no interchain association/aggregation.[18] Otherwise, the scattering intensity would increase significantly because it is proportional to the square of the mass of a scattering object. In order to study the kinetics of phase transition from the dilute regime to the semidilute regime with a good signal-to-noise ratio, we decided to use a water-soluble fluorescent probe, ANS, to follow the phase transition of PNIPAM. Figure 3 shows the fluorescence spectra of ANS (118 μM) in a PNIPAM-2 aqueous solution (5×10^{-4} g/mL) at three different temperatures. Note that ANS has been widely used to study both the folding kinetics and hydrophobic sites of protein chains because of its characteristic nonfluorescence in water but high fluorescence in organic solvents or when enwrapped by hydrophobic sites of proteins.[27,37−41] Figure 3 shows that the fluorescence intensity of ANS increases with the solution temperature in the presence of PNIPAM and λ_{max} of the ANS fluorescence spectra shifted from 517 to 472 nm when the PNIPAM solution was heated, which is consistent with the results described by Tirrell and Schild.[41] The temperature dependence of the ANS fluorescence intensity at 472 nm is summarized in the inset of Figure 3. It shows that when the temperature is lower than the lower critical solution temperature (LCST) $\sim$ 31.4 °C, the fluorescence intensity is a constant and sharply increases and levels off to a maximum only within ~2 °C when the temperature is higher than the LCST. The change of the ANS fluorescence
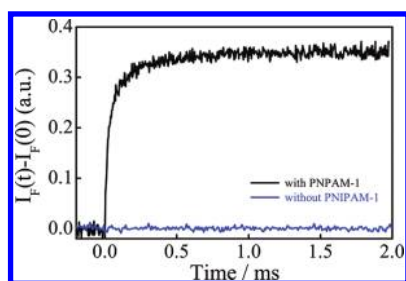
Figure 4. Time dependence of fluorescence intensity changes of ANS in aqueous solution after an infrared laser heating pulse, respectively, with and without PNIPAM-1, where the intensity of the infrared pulsed light was 6.5 mJ, the concentrations of PNIPAM-1 and ANS were 1.81 mg/mL and 118 μM, respectively, and the initial temperature before the heating was 30.4 °C.
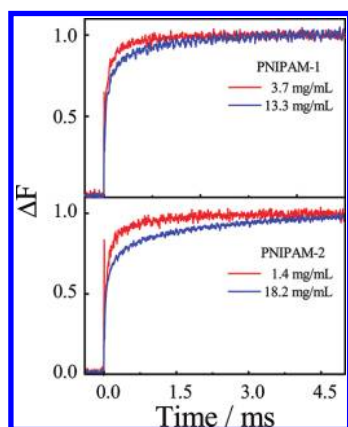

Figure 5. Time dependence of fluorescence intensity changes (ΔF) from PNIPAM aqueous solution after the laser-induced temperature jump at different concentrations, where ΔF is defined as $[I_F(t) - I_F(0)]/[I_F(max) - I_F(0)]$.

intensity is well-correlated to the microenvironmental change induced by the phase transition of linear PNIPAM chains.

Figure 4 shows the time dependence of fluorescence intensity changes of ANS in aqueous solution after an infrared laser heating pulse, with and without PNIPAM-1, respectively. It is clear that the ANS fluorescence intensity remains a constant without PNIPAM in the solution after the heating induced the infrared laser pulse. This is expected because we investigated the temperature dependence of the ANS fluorescence intensity in aqueous solution without PNIPAM in a static fashion in the temperature range of 18−41 °C and found that the ANS fluorescence intensity is independent of the solution temperature. Figure 4 shows that with PNIPAM, the ANS fluorescence intensity increases rapidly in the first 0.5 ms and levels off after several milliseconds. It should be noted that the observed signal is much broader than the pulse width of the infrared laser (∼10 ns); thus, the signal cannot be due to the laser pulse used to irradiate the sample.

Figure 5 shows the initial time-dependence of the fluorescence intensity after the solution was irradiated with the same laser power (6.5 mJ) that can lead to a temperature jump of ∼3 °C. Note that keeping the power of the infrared heating laser pulse at 6.5 mJ during the whole experiment is important because it is well-known that the phase transition slows down when quenching depth is decreased.[18] We also find the changes of the fluorescence
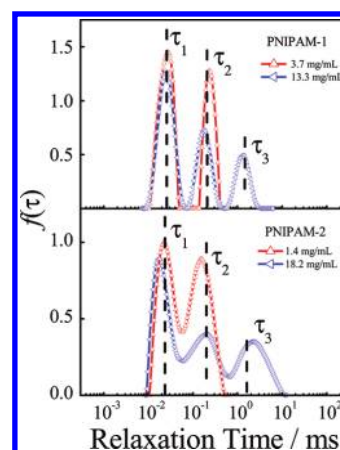

Figure 6. The relaxation time distribution for PNIPAM aqueous solution at different concentrations fit by CONTIN.

intensity became slow at higher concentration. In order to process the data, continuous distributions of exponentials (CONTIN program) provided by Provencher[42,43] and double or triple exponential functions have been used. CONTIN program is used first to analyze the data, because it has the ability to resolve multimodal relaxation distribution under favorable conditions without information on the components. CONTIN provides the distribution of relaxation times τ, $f(\tau)$, as the inverse Laplace transform of the $(1 - \Delta F)$ function

$$1 - \Delta F = 1 - \frac{I(t) - I(0)}{I(\max) - I(0)} = \int_0^\infty f(\tau)e^{-t/\tau} \, d\tau \qquad (1)$$

where $I(t)$ and $I(0)$ are the fluorescence intensities at time $t = t$ and $t = 0$, and $I(\max)$ is the maximum fluorescence intensities. Figure 6 shows the relaxation time distribution corresponding to the data in Figure 5 analyzed by the CONTIN program. For both PNIPAM-1 and PNIPAM-2 samples, there are two relaxation times when the concentration of PNIPAM is low, and an extra (third) peak arises when the concentration is higher, which means that these curves can be reasonably fit by a double- or a triple-exponential function

$$1 - \Delta F = 1 - \frac{I(t) - I(0)}{I(\max) - I(0)} = a_1 e^{-t/\tau_1} + a_2 e^{-t/\tau_2}$$

or

$$1 - \Delta F = 1 - \frac{I(t) - I(0)}{I(\max) - I(0)}$$

$$= a_1 e^{-t/\tau_1} + a_2 e^{-t/\tau_2} + a_3 e^{-t/\tau_3} \qquad (2)$$

where τ_1, τ_2, and τ_3 are characteristic relaxation times of three processes, respectively, $a_1 + a_2 = 1$ or $a_1 + a_2 + a_3 = 1$. From Figure 6, we know that the characteristic relaxation times of the three processes are ∼25 μs, ∼200 μs, and ∼1.5 ms, respectively. In our previous study, we concluded that in PNIPAM dilute solution there exist two characteristic transition times less than 1 ms, τ_{pearls} (∼0.1 ms) and $\tau_{coarsening}$ (∼0.8 ms).[18] The faster characteristic relaxation time here can be attributed to the deeper quench in our present experiment (∼3 °C) than that in the previous study (∼2 °C). Because of the ill-posed nature of eq 1 in the presence of noise, we decided to analyze all the data by using a nonlinear least-squares fitting with double or triple exponential decay functions, as shows in eq 2. On the basis of the results from CONTIN analyses,
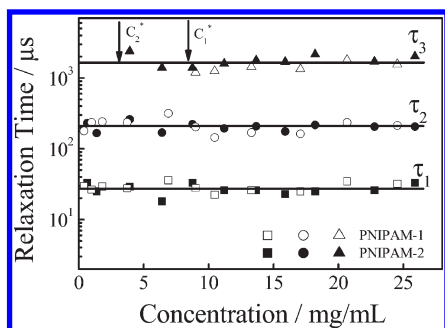
Figure 7. PNIPAM concentration dependence of characteristic times of the three relaxation determined by eq 2, where the intensity of the infrared pulsed light was 6.5 mJ and the concentration of ANS was 118 μM.

Figure 9. Schematic diagram of the kinetics of phase transition of PNIPAM in semidilute solution.
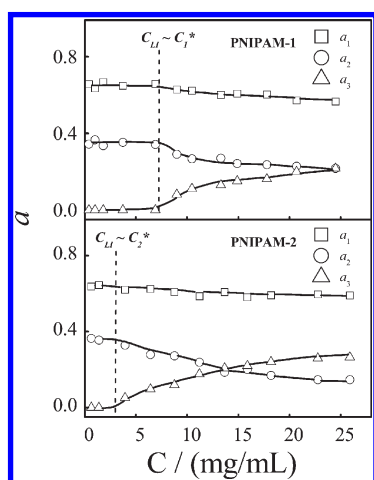

Figure 8. PNIPAM concentration dependence of contributions from the each component, where the intensity of the infrared pulsed light was 6.5 mJ and the concentration of ANS was 118 μM.

first we use nonlinear least-squares fitting with four parameters for double exponential decay to obtain a_1, a_2 and τ_1, τ_2. When the fitting residuals become obviously higher, we use six parameters for triple exponential decay to obtain a_1, a_2, a_3 and τ_1, τ_2, τ_3. By this method we can find the value of the three relaxation times at different concentrations, which are shown in Figure 7.

It is well-known that when the polymer concentration is at the so-called overlap concentration (C^*), polymer chains touch each other.[44] C^* can be calculated quantitatively by $C^* \sim 3M/(4\pi N_A R_g^3)$, where M is the molecular weight of the polymer, N_A is Avogadro's number, and R_g is the radius of gyration of the polymer chain. From the data determined by laser light scattering in Table 1, the overlap concentrations of PNIPAM-1 and PNIPAM-2 are $C_1^* \sim 7.0$ mg/mL and $C_2^* \sim 3.4$ mg/mL, respectively. From Figure 7, we know the third process arises when the concentration of PNIPAM is higher than its overlap concentration. All of these three characteristic relaxation times are nearly independent of PNIPAM concentration and are $\sim$25 μs, $\sim$200 μs, and $\sim$1.5 ms, respectively, which are consistent with the results analyzed by CONTIN. For the two faster relaxations, we have observed the same phenomenon in our previous experiments, that is, the chain-length-independent first stage may be attributed to the nucleation and initial growth of some pearls and the second slower proce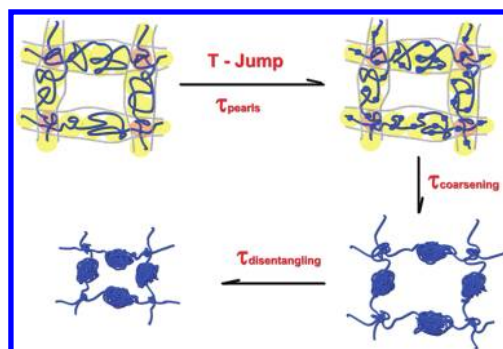ss is related to the merging and coarsening of the pearls. We set the three characteristic relaxation times as 25 μs, 200 μs, and 1.5 ms and use a double- or triple-exponential function to fit the data in order to evaluate the contribution from each component. PNIPAM concentration dependence on the contribution of the three processes is shown in Figure 8. From Figure 8 we know that there is no contribution from the third process (a_3) under certain concentration (C_{LI}) and then it gradually increases with the PNIPAM concentration. At the same time, the contribution of the second process (a_2) decreases with increasing PNIPAM concentration above C_{LI}. It is interesting to find that C_{LI} is very close to C^*, which indicates that overlapping of polymers influences the kinetics of phase transition of PNIPAM chains when the PNIPAM concentration increases. Here we propose an explanation based on blob model: before the semidilute PNIPAM aqueous solution was heated by the ultrafast infrared laser pulse, the solution can be treated as in Θ solvent, because we set the temperature as $\sim$30.4 °C and at this time the entire solution is filled with blobs.[44] The adjacent blobs around a given blob could be from the same or different polymer chains.[44] After the laser pulse heated the solution, the solvent quality changed from Θ to poor instantly. Some monomers in the blobs start to form pearls within each blob. Note that there is only a small chance for monomers of other blobs to sneak in a blob to form pearls; the formation of pearls takes place inside individual blobs which is nearly independent of the concentration of the solution. Thus, the characteristic relaxation time (τ_1) and the contribution of this process (a_1) changes little with PNIPAM concentration. Because of the existence of the entanglement in semidilute solution, the further process is complicated. A contribution for the third relaxation time can only be probed at PNIPAM concentrations larger than the overlap concentration C^*. This result suggests that it is due to interactions between different PNIPAM chains in semidilute regime. Hence, we have proposed a new method to study the interpenetration of polymer chains in solution and determine the overlap concentration of PNIPAM chains. One advantage of this method is that the amount of PNIPAM sample needed is $\sim$10 mg, which is smaller compared to other methods, like viscosity measurements and laser light scattering method. Note that in the present study, this new method is only suitable for thermally sensitive polymers in aqueous solutions. Figure 9 schematically summarizes the phase transition diagram of the kinetics of phase transition of homopolymers in semidilute solution after the heating laser pulse. In semidilute solution, the PNIPAM homopolymer chains overlapped with other chains, but for the most part, the chains are individual, not overlapped. When the solution

12005

dx.doi.org/10.1021/jp204853p |*J. Phys. Chem. B* 2011, 115, 12001–12006

is heated, the polymer undergoes three distinct kinetic stages with three characteristic transition times: τ_{pearls} ($\sim$0.02 ms) for the formation of the pearls on the chain and $\tau_{\text{coarsening}}$ ($\sim$0.2 ms) for the growth and packing of the pearls. The third process [$\tau_{\text{disentangling}}$ ($\sim$1.5 ms)] can only be found in the semidilute regime. This is because the "coarsened pearls" formed by the collapsed polymer chains needed further growth, which disentangled the polymer chains at the overlapped points.

CONCLUSION

Our results have revealed that there exist two characteristic transition times in dilute regime, namely, τ_{pearls} ($\sim$0.02 ms) for the formation of the pearls on the chain and $\tau_{\text{coarsening}}$ ($\sim$0.2 ms) for the growth and packing of the pearls. When the concentration is higher than the overlap concentration, a third process, $\tau_{\text{disentangling}}$ ($\sim$1.5 ms), arises and the contribution from this process increases with the PNIPAM concentration. The third process may be due to the disentanglement of the overlapped points. Here we provide a new way to detect the inhomogeneity of the chain segments.

AUTHOR INFORMATION

Corresponding Author
*E-mail: xdye@ustc.edu.cn.

ACKNOWLEDGMENT

REFERENCES

(1) Melnikov, S. M.; Sergeyev, V. G.; Yoshikawa, K. *J. Am. Chem. Soc.* **1995**, *117*, 2401–2408.
(2) Melnikov, S. M.; Sergeyev, V. G.; Yoshikawa, K. *J. Am. Chem. Soc.* **1995**, *117*, 9951–9956.
(3) Yoshikawa, K.; Takahashi, M.; Vasilevskaya, V. V.; Khokhlov, A. R. *Phys. Rev. Lett.* **1996**, *76*, 3029–3031.
(4) Sali, A.; Shakhnovich, E.; Karplus, M. *Nature* **1994**, *369*, 248–251.
(5) Abkevich, V. I.; Gutin, A. M.; Shakhnovich, E. I. *Biochemistry* **1994**, *33*, 10026–10036.
(6) Winnik, F. M. *Macromolecules* **1990**, *23*, 233–242.
(7) Ringsdorf, H.; Venzmer, J.; Winnik, F. M. *Macromolecules* **1991**, *24*, 1678–1686.
(8) Schild, H. G. *Prog. Polym. Sci.* **1992**, *17*, 164–249.
(9) Wu, C.; Zhou, S. Q. *Macromolecules* **1995**, *28*, 8381–8387.
(10) Wu, C.; Zhou, S. Q. *Macromolecules* **1995**, *28*, 5388–5390.
(11) Wu, C.; Zhou, S. Q. *Phys. Rev. Lett.* **1996**, *77*, 3053–3055.
(12) Ye, X. D.; Ding, Y. W.; Li, J. F. *J. Polym. Sci. Part B: Polym. Phys.* **2010**, *48*, 1388–1393.
(13) Xu, J.; Zhu, Z. Y.; Luo, S. Z.; Wu, C.; Liu, S. Y. *Phys. Rev. Lett.* **2006**, *96*, 027802–1−027802–4.
(14) Hu, J. M.; Wang, D.; Xu, J.; Zhu, Z. Y.; Liu, S. Y. *Macromol. Chem. Phys.* **2010**, *211*, 2573–2584.
(15) Yushmanov, P. V.; Fuor, I.; Iliopoulos, I. *Macromol. Chem. Phys.* **2006**, *207*, 1972–1979.
(16) Tsuboi, Y.; Yoshida, Y.; Kitamura, N.; Iwai, K. *Chem. Phys. Lett.* **2009**, *468*, 42–45.
(17) Zhang, S. H.; Chen, Y.; Li, H.; Weng, Y. X. *Chin. J. Chem. Phys.* **2009**, *22*, 447–452.
(18) Ye, X. D.; Lu, Y. J.; Shen, L.; Ding, Y. W.; Liu, S. L.; Zhang, G. Z.; Wu, C. *Macromolecules* **2007**, *40*, 4750–4752.
(19) Ding, Y. W.; Zhang, G. Z. *Macromolecules* **2006**, *39*, 9654–9657.
(20) Ding, Y. W.; Ye, X. D.; Zhang, G. Z. *J. Phys. Chem. B* **2008**, *112*, 8496–8498.
(21) Yuan, G. C.; Wang, X. H.; Han, C. C.; Wu, C. *Macromolecules* **2006**, *39*, 6207–6209.
(22) Tao, F. F.; Wang, X. L.; Che, B.; Zhou, D. S.; Chen, W.; Xue, Q.; Zou, D. W.; Tie, Z. X. *Macromol. Rapid Commun.* **2008**, *29*, 160–164.
(23) Tao, F. F.; Han, J. L.; Gu, Q.; Teng, C.; Zou, D. W.; Zhou, D. S.; Xue, G. *Macromolecules* **2008**, *41*, 9890–9895.
(24) Irondi, K.; Zheng, M. Z.; Duhamel, J. *J. Phys. Chem. B* **2006**, *110*, 2628–2637.
(25) Mathew, A.; Siu, H.; Duhamel, J. *Macromolecules* **1999**, *32*, 7100–7108.
(26) Duhamel, J. *Acc. Chem. Res.* **2006**, *39*, 953–960.
(27) Stryer, L. *Science* **1968**, *162*, 526–533.
(28) Zhou, S. Q.; Fan, S. Y.; Au-yeung, S. T. F.; Wu, C. *Polymer* **1995**, *36*, 1341–1346.
(29) Ye, X. D.; Lu, Y. J.; Liu, S. L.; Zhang, G. Z.; Wu, C. *Langmuir* **2007**, *23*, 10366–10371.
(30) Kazzaz, A.; Ruschin, S.; Shoshan, I.; Ravnitsky, G. *IEEE J. Quantum Electron* **1994**, *30*, 3017–3024.
(31) Williams, A. P.; Longfellow, C. E.; Freier, S. M.; Kierzek, R.; Turner, D. H. *Biochemistry* **1989**, *28*, 4283–4291.
(32) Palmer, K. F.; Williams, D. *J. Opt. Soc. Am.* **1974**, *64*, 1107–1110.
(33) Wang, X. H.; Qiu, X. P.; Wu, C. *Macromolecules* **1998**, *31*, 2972–2976.
(34) Ding, Y. W.; Ye, X. D.; Zhang, G. Z. *Macromolecules* **2005**, *38*, 904–908.
(35) Cheng, H.; Shen, L.; Wu, C. *Macromolecules* **2006**, *38*, 2325–2329.
(36) Lu, Y. J.; Zhou, K. J.; Ding, Y. W.; Zhang, G. Z.; Wu, C. *Phys. Chem. Chem. Phys.* **2010**, *12*, 3188–3194.
(37) Stryer, L. *J. Mol. Biol.* **1965**, *13*, 482–495.
(38) Brand, L.; Gohlke, J. R.; Rao, D. S. *Biochemistry* **1967**, *6*, 3510–3518.
(39) Semisotnov, G. V.; Rodionova, N. A.; Razgulyaev, O. I.; Uversky, V. N.; Gripas, A. F.; Gilmanshin, R. I. *Biopolymers* **1991**, *31*, 119–128.
(40) Itzhaki, L. S.; Evans, P. A.; Dobson, C. M.; Radford, S. E. *Biochemistry* **1994**, *33*, 5212–5220.
(41) Schild, H. G.; Tirrell, D. A. *Langmuir* **1991**, *7*, 1319–1324.
(42) Provencher, S. W. *Comp. Phys.* **1982**, *27*, 213–227.
(43) Provencher, S. W. *Comp. Phys.* **1982**, *27*, 229–242.
(44) Teraoka, I. *Polymer Solutions: An Introduction to Physical Properties*; John Wiley & Sons, Inc.: New York, 2002.